Supplementary Material (ESI) for Molecular BioSystems

Supporting Information for:

Using a genetically targeted sensor to investigate the role of presenilin-1 in ER Ca^{2+} levels and dynamics

Janet E. McCombs [1], Emily A. Gibson [2], Amy E. Palmer [1*]

Supplementary Methods
Supplementary Figure S1: **Demonstration of gamma-secretase activity in MEF cells.**
Supplementary Figure S2: **The effect of PS1 on ATP-induced ER Ca^{2+} release.**
Supplementary Figure S3: **Analysis of oscillation data using IGOR Pro.**

Supplementary Methods

Cloning and constructs

To confirm gamma-secretase activity in individual cells, a fluorescently-tagged APP substrate (termed C99-mCherry) was designed. C99-mCherry was generated by PCR amplification of the APP signal sequence (residues 1 – 21) and its post β-secretase cleaved C-terminus (residues 653 – 751) from Gene Pool™ cDNA Human Normal Adult Brain library (Invitrogen). The signal sequence was ligated between HindIII and KpnI into the multiple cloning site of pcDNA3 (Invitrogen). The C99-APP fragment was subsequently ligated into the same vector between KpnI and NotI. The mCherry fluorescent protein was ligated into the APP-pcDNA3 vector between NotI and XbaI in order to tag the C-terminus of C99-APP.

Aβ ELISA

MEF cells were doubly transfected with full-length APP and PS1 mutants 72 hours prior to carrying out the assay and media was changed 18 hours post-transfection. Analysis was performed using the BetaMark x-40 and BetaMark x-42 ELISA Kits (Covance). Secreted Aβ protein in the media was concentrated using Amicon Ultra 3K centrifugal filter devices (Millipore). Samples diluted 1:2 in working incubation buffer were run in duplicate according to manufacturer recommended protocol.

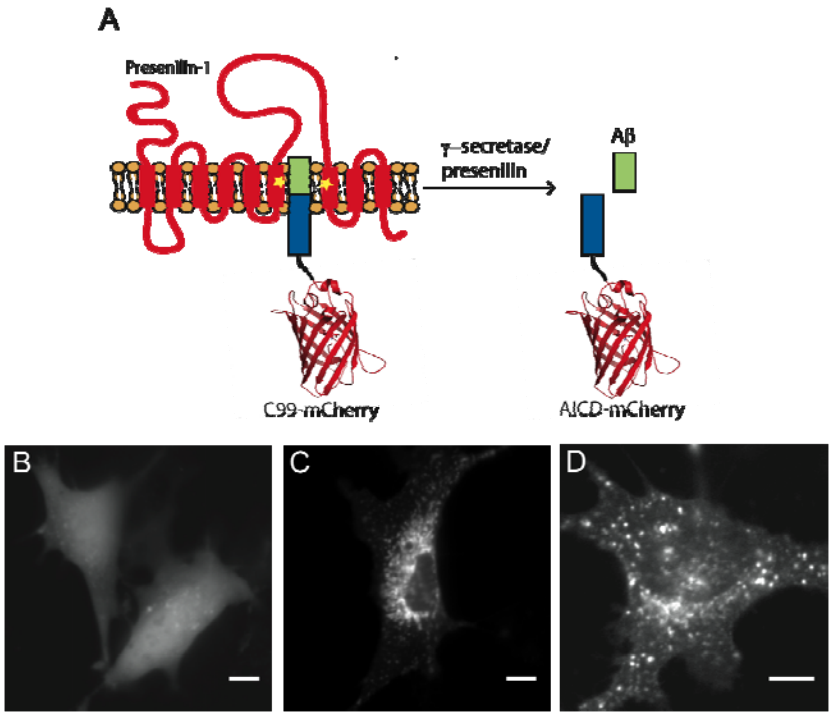

Figure S1. Demonstration of gamma-secretase activity in MEF cells. (A) Schematic representation of the C99-mCherry probe consisting of post-β-secretase cleaved APP with the mCherry fluorophore on its C-terminus. Upon recognition by the gamma-secretase complex, PS cleaves the probe into its intracellular domain (AICD) and Aβ fragments. (B) The C99-mCherry probe in WT MEF cells displaying diffuse cytosolic fluroescence. (C) WT MEF cells treated with the gamma-secretase inhibitor DAPT and expressing the C99-mCherry probe displaying punctate fluorescence. (D) DKO MEF cells expressing the C99-mCherry probe. Fluorescence is comparable to WT + DAPT cells, as there is no PS and thus no cleavage of the probe in cells. Scale bar is 10μm.

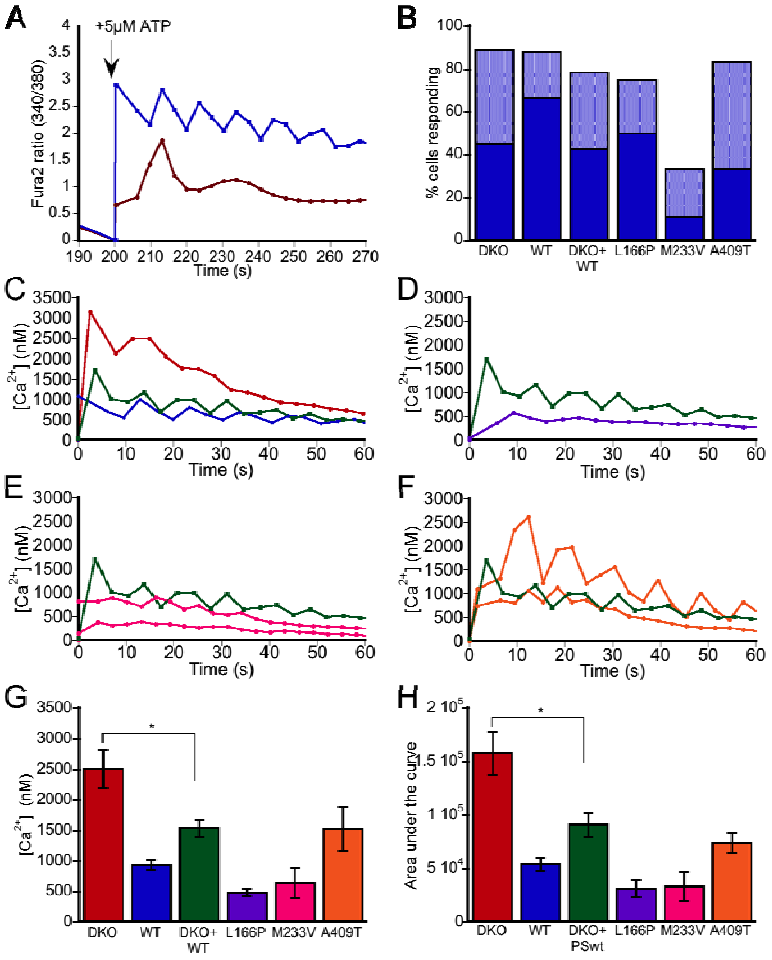

Figure S2. The effect of PS1 on ATP-induced ER Ca^{2+} release. (A) Upon treatment with ATP, Ca^{2+} release from cells either occurred immediately (blue) or displayed a noticeable delay (red), with a comparatively smaller Ca^{2+} response. (B) Percent of responding cells that showed immediate (dark blue) or delayed (light blue) Ca^{2+} release. Cells showed similar responsiveness (~ 80%) except for DKO + M233V, which had decreased ATP sensitivity. WT: n = 42; DKO: n = 56; DKO + WT: 14; L166P: n = 8; M233V: n = 18; A409T: n = 12. (C – F) Representative oscillation curves for the amount of Ca^{2+} released in immediately responding cells for DKO (red), WT (blue) and DKO + WT (green); (D – F) Comparison of the amount of Ca^{2+} released upon stimulation with ATP for DKO + WT (green) versus L166P (purple; D), M233V (pink; E), and A409T (orange; F). (G) Maximum $[Ca^{2+}]$ peak heights upon addition of 5μM ATP. Asterisk: $P < 0.05$, ANOVA with Student-Newman-Keuls post-hoc test. WT: n = 27; DKO: n = 25; DKO + WT: n = 6; L166P: n = 3; M233V: n = 2; A409T: n = 4. (H) Amount of Ca^{2+} released from the ER upon ATP treatment. Data represent area under the oscillation curve. DKO cells released more Ca^{2+} upon stimulation with ATP than DKO + WT, consistent with levels of ER Ca^{2+}. However, though not significant, L166P appeared to release less Ca^{2+} upon treatment with ATP though the ER concentration of Ca^{2+} was similar to WT. M233V also appeared to release less Ca^{2+} than WT, consistent with the lower level of ER Ca^{2+}, though differences were not significant. Interestingly, the Ca^{2+} response for the A409T mutant was similar to WT despite

this mutant having a lower ER Ca^{2+} load. Asterisk: $P < 0.05$, ANOVA with Student-Newman-Keuls post-hoc test. Error bars indicate SEM.

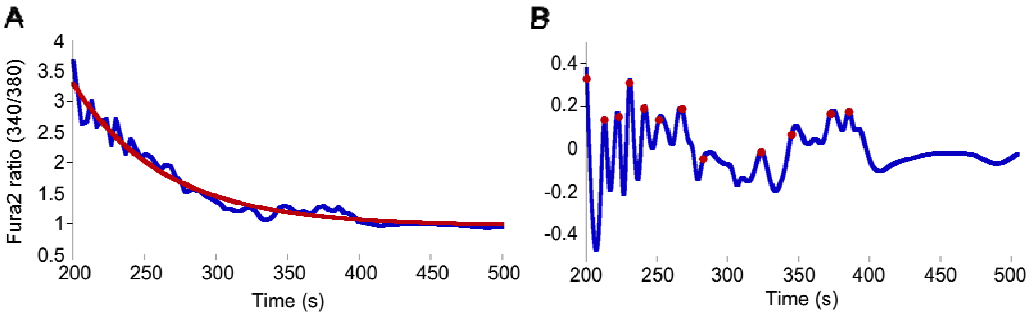

Figure S3. Analysis of oscillation data using IGOR Pro. (A) Representative oscillation curve (blue) fit to an exponential decay (red), $A(t) = A_0 e^{-(t - t_0)k}$. (B) The exponential decay fit from *A* is subtracted from the oscillation curve to enhance the peaks. Peak values (depicted by red dots) are determined using the Peak AutoFind macro in IGOR Pro.